THE JOURNAL OF BIOLOGICAL CHEMISTRY VOL. 280, NO. 37, pp. 32389–32397, September 16, 2005

A New Type of Bacteriophytochrome Acts in Tandem with a Classical Bacteriophytochrome to Control the Antennae Synthesis in *Rhodopseudomonas palustris*[*]

Received for publication, June 24, 2005, and in revised form, July 11, 2005 Published, JBC Papers in Press, July 11, 2005, DOI 10.1074/jbc.M506890200

Eric Giraud[‡1], Sébastien Zappa[§1], Laurie Vuillet[‡], Jean-Marc Adriano[§], Laure Hannibal[‡], Joël Fardoux[‡], Catherine Berthomieu[§], Pierre Bouyer[§], David Pignol[§], and André Verméglio[§2]

*From the [‡]Laboratoire des Symbioses Tropicales et Méditerranéennes, IRD, CIRAD, AGRO-M, INRA, UM2, TA 10/J, Campus de Baillarguet, 34398 Montpellier Cedex 5, France and [§]*CEA/*Cadarache DEVM-Laboratoire de Bioénergétique Cellulaire UMR 6191 CNRS-CEA, Aix-Marseille II 13108 Saint Paul lez Durance Cedex, France*

Phytochromes are chromoproteins found in plants and bacteria that switch between two photointerconvertible forms via the photoisomerization of their chromophore. These two forms, Pr and Pfr, absorb red and far-red light, respectively. We have characterized the biophysical and biochemical properties of two bacteriophytochromes, *Rp*BphP2 and *Rp*BphP3, from the photosynthetic bacterium *Rhodopseudomonas palustris*. Their genes are contiguous and localized near the *pucBAd* genes encoding the polypeptides of the light harvesting complexes LH4, whose synthesis depends on the light intensity. At variance with all (bacterio)phytochromes studied so far, the light-induced isomerization of the chromophore of *Rp*BphP3 converts the Pr form to a form absorbing at shorter wavelength around 645 nm, designated as Pnr for *n*ear *r*ed. The quantum yield for the transformation of Pr into Pnr is about 6-fold smaller than for the reverse reaction. Both *Rp*BphP2 and *Rp*BphP3 autophosphorylate in their dark-adapted Pr forms and transfer their phosphate to a common response regulator Rpa3017. Under semi-aerobic conditions, LH4 complexes replace specifically the LH2 complexes in wild-type cells illuminated by wavelengths comprised between 680 and 730 nm. In contrast, mutants deleted in each of these two bacteriophytochromes display no variation in the composition of their light harvesting complexes whatever the light intensity. From both the peculiar properties of these bacteriophytochromes and the phenotypes of their deletion mutants, we propose that they operate in tandem to control the synthesis of LH4 complexes by measuring the relative intensities of 645 and 710 nm lights.

Phytochromes are biliprotein photoreceptors originally discovered in plants (1, 2) but only recently in bacteria (3–6). They respond to red/far-red light via a reversible shift from a red absorbing form (Pr) to a far-red absorbing form (Pfr). These light sensors regulate many aspects of photomorphogenesis in plants (1, 2). In bacteria, they have been also described to play various roles, control of the light harvesting complexes in *Fremyella diplosiphon* (3), regulation of chalcone synthase in *Rhodospirillum centenum* (5), regulation of carotenoid synthesis in *Deinococcus radiodurans* (6), phototaxis in *Synechocystis* (7), and control of photosystem synthesis in *Bradyrhizobium* and *Rhodopseudomonas* (*Rds.*)[3] *palustris* (8). Based upon primary sequence alignment, phytochromes and bacteriophytochromes possess a similar protein organization with an N-terminal chromophore binding domain (CBD) and a C-terminal module involved in signal transduction and dimerization. The plant and cyanobacteria chromophores are 3E-phytochromobilin and 3Z-phycocyanobilin, respectively (1, 9), whereas other proteobacteria use, as chromophore, biliverdin, the simplest linear tetrapyrrole synthesized from heme by a heme oxygenase (10). Like plant phytochromes, most bacteriophytochromes studied so far contain a two-component histidine kinase motif at their C termini. However some exceptions occur such as the bacteriophytochromes of the photosynthetic bacteria *Bradyrhizobium* (*Br*BphP) and *Rps. palustris* (denoted here *Rp*BphP1), which do not possess a histidine kinase motif but an S-box domain that might be involved in protein-protein interactions (8). Photoconversion of these two bacteriophytochromes from their Pfr to Pr form triggers the synthesis of the entire photosynthetic apparatus and the associated bacteriochlorophyll and carotenoid molecules (8, 11, 12). This photosynthetic apparatus is composed of a photochemical reaction center and of light-harvesting (LH) complexes. The photosynthetic apparatus of *Rps. palustris* presents the peculiarity of possessing several peripheral LH complexes, encoded by distinct *pucBA* genes (13). The relative proportion of these LH complexes varies according to the light environment (14, 15). They differ by their absorption properties and carotenoid content. Some of these complexes present two distinct optical transitions absorbing around 800 and 850 nm in the near infrared. They are named LH2 (or B800–850 LH2) to differentiate them from the LH1 complexes, which present a single broad absorption band around 870 nm. A novel type of LH, recently characterized and designated LH4 (or B800 LH2), is expressed under low light intensity and presents a single absorption band in the near infrared centered at 800 nm (15).

The recent sequencing of the complete genome of *Rps. palustris* strain CGA009 revealed, in addition to *RpBphP1*, the unexpected presence of five other putative bacteriophytochrome genes scattered over the genome (16). This suggests that this bacterium has developed a sophisticated and complex network of photoreceptors for its adaptation to light environment. Four of these bacteriophytochromes genes, *RpBphP1* (*rpa1537*), *RpBphP2* (*rpa3015*), *RpBphP3* (*rpa3016*), and *RpBphP4* (*rpa1490*), are located close to photosynthesis genes. The *RpBphP1* gene is found inside the photosynthesis gene cluster, and, as already stated, its product controls the synthesis of the RC-LH1 core complexes (8). The *RpBphP4* gene is located close to the *pucBAe* genes encoding one of the

[*] This work was supported by the CEA, the IRD, and the CNRS (programme Protéomique). The costs of publication of this article were defrayed in part by the payment of page charges. This article must therefore be hereby marked "*advertisement*" in accordance with 18 U.S.C. Section 1734 solely to indicate this fact.

[1] Both authors contributed equally to this study.

[2] To whom correspondence should be addressed. Tel.: 33-442254630; Fax: 33-442254701; E-mail: avermeglio@cea.fr.

[3] The abbreviations used are: *Rds.*, *Rhodopseudomonas*; CBD, chromophore binding domain; LED, light-emitting diode; LH, light harvesting; FTIR, Fourier transform infrared spectroscopy.

LH2 complexes. Remarkably, the *RpBphP2* and *RpBphP3* genes are organized in tandem downstream the *pucBAd* encoding the apoproteins of the LH4 complexes. Two other genes coding for LH complexes (the *pucBAc* genes *rpa3009* and *rpa3010*) are located upstream the *pucBAd* genes. However, one of them, *pucAc*, contains a frameshift mutation and has been annotated as a pseudogene (16).

To better understand the role and function of these bacteriophytochromes in the adaptation of *Rps. palustris* to changes in its light environment, we initiated their systematic study at the genetic and biochemical level. Of particular interest are the two bacteriophytochromes, *Rp*BphP2 and *Rp*BphP3. What is the significance of the tandem organization of the two bacteriophytochromes genes? Do these two bacteriophytochromes possess different properties? Are these two bacteriophytochromes involved in the regulation of the closely located *pucBAd* genes or in different regulatory processes? In this report, we show by combining genetics, biochemical and biophysical approaches that the bacteriophytochrome *Rp*BphP3 possesses unusual photochemical properties and works in tandem with *Rp*BphP2 to regulate the synthesis of the LH4 complexes.

MATERIALS AND METHODS

Bacterial Strains and Growth Conditions—*Rps. palustris* CEA001 strain (11) was grown under semiaerobic conditions for 72 h at 30 °C on Petri dishes filled with 40% Sistrom-agar medium and sealed with tape. The cells were subjected to continuous illumination provided by a series of light-emitting diodes (LEDs) of different wavelengths between 590 and 875 nm. Each LED illuminated a 3.5 cm^2 area. The half-peak bandwidth was below 25 nm for all wavelengths. Irradiance was adjusted between 1 and 200 μmol of photon/m^2/s.

Expression and Purification of Rpa3014, RpBphP2, RpBphP3, and Rpa3017 Proteins—The *rpa3014*, *RpBphP2*, *RpBphP3*, and *rpa3017* genes were amplified by polymerase chain reaction from genomic DNA of *Rps. palustris* CEA001 using primers designed to add appropriate restriction sites for expression as His_6-tagged versions in pBAD/HisB expression vector (Invitrogen). To reconstitute *in vivo* the *Rp*BphP2 and *Rp*BphP3 holobacteriophytochromes, the *hmuO* gene from *Bradyrhizobium* ORS278 was amplified by polymerase chain reaction using primers designed to add a ribosome binding site upstream the gene and restriction site for insertion in the previous constructions pBAD::*RpBphP2* and pBAD::*RpBphP3*. The recombinant proteins were overexpressed in *Escherichia coli* LMG194 and purified as described previously (11).

Protein Kinase Assays—Protein kinase reaction was performed as described previously (9). For autophosphorylation experiments, the bacteriophytochromes *Rp*BphP2 or *Rp*BphP3 were either dark-adapted for more than 1 h or pre-illuminated with saturating red light (705 nm) at 30 °C. The kinase reactions were initiated by adding [γ-^{32}P]ATP, and the resulting mixtures were subjected to a further 1-h darkness condition or illumination. At this stage, the reactions were stopped by addition of the buffer used for the SDS-PAGE assay and analyzed by gel electrophoresis. For the phosphotransfer experiments, the *Rp*BphP2 and *Rp*BphP3 were incubated in the presence of [γ-^{32}P]ATP during 1 h in the dark or under 705 nm light and for an additional 10 min with equal amount of Rpa3014 or Rpa3017 or a mixture of Rpa3014 and Rpa3017. ^{32}P-Labeled products were quantified by using a Typhoon PhosphorImager (Amersham Biosciences).

Construction of RpBphP2 and RpBphP3 Mutant Strains—For the construction of the *Rp*BphP2 null mutant, a 1.4-kb PstI fragment inside the *RpBphP2* gene was deleted and replaced by the *lac*Z-Km^r cassette of pKOK5 (17). The *RpBphP3* null mutant was obtained by the deletion of a 0.5-kb SalI fragment inside the *RpBphP3* gene and replacement by the *lac*Z-Km^r cassette. These constructions were introduced in the pJQ200 suicide vector (18) and delivered by conjugation into the *Rps. palustris* CEA001 strain as described (11). Double recombinants were selected on sucrose and confirmed by polymerase chain reaction.

Absorbance Spectra Measurements—Absorbance spectra of purified *Rp*BphP2 and *Rp*BphP3 bacteriophytochromes were recorded with a Cary 50 spectrophotometer. Bacteriophytochrome spectra were recorded either in the dark or under continuous illumination at 645, 705, or 750 nm provided by LEDs with an irradiance of 15 μmol of photon/m^2/s. Light-induced absorbance changes were performed with a laboratory-built spectrophotometer similar to the one developed by Joliot *et al.* (19). The absorption level is sampled using 2-μs monochromatic flashes given from 1 ms to several seconds after actinic excitation. Actinic illumination was provided by a Xenon flash (2 μs).

Fluorescence Measurements—Fluorescence measurements have been performed at room temperature using a Cary Eclipse spectrophotometer. To perform the photoinduced transition of *Rp*BphP2 and *Rp*BphP3, excitation light was provided by 645-, 705-, or 750-nm LEDs with an irradiance of 15 μmol of photon/m^2/s. For the measurement of the excitation spectra (2-nm slit bandwidth), the fluorescence was detected at 730 nm (10-nm slit bandwidth). For the emission spectra (2-nm slit bandwidth), the excitation was set at 400 nm (10-nm slit bandwidth). Measurements of the variation of the fluorescence yield were performed at 400 nm for the excitation wavelength (10-nm slit bandwidth) and 730 nm for the emission wavelength (2-nm slit bandwidth).

Light-induced FTIR Difference Spectra Measurements—Light-induced FTIR difference spectra were recorded at 10 °C at 4 cm^{-1} resolution, with a Bruker 66 SX spectrometer equipped with a KBr beam splitter and nitrogen-cooled MCT-A detector. The FTIR samples consisted in 10 μl of a solution of bacteriophytochrome at a concentration of ≈200 μM, in 50 mM Tris-HCl, pH 8, 100 mM KCl, 20 mM $MgCl_2$, deposited between two calcium fluoride windows sealed with silicon grease to avoid sample dehydration. The samples were subjected to successive light cycles, applying 705 nm light to generate Pfr (or Pnr) and 750 or 645 nm light to restore the Pr form of *Rp*BphP2 or *Rp*BphP3, respectively.

RESULTS

Expression and Purification of Recombinant Holobacteriophytochromes—The *RpBphP2* and *RpBphP3* genes belong to the same putative operon, which includes three other putative response regulator genes (*rpa3014*, *rpa3017*, and *rpa3018*) (Fig. 1*A*). This operon is found upstream the *pucBAd* genes encoding the apoproteins of the light-harvesting complexes LH4. Sequence analysis reveals that the *Rp*BphP2 and *Rp*BphP3 proteins are highly homologous, with 54% of sequence identity and 76% similarity. In contrast, they present only 30–35% sequence identity with the other bacteriophytochromes of *Rps. palustris*. These two bacteriophytochromes display the classical bacteriophytochrome architecture with an N-terminal CBD and a C-terminal histidine kinase domain (Fig. 1*B*). To prove that *RpBphP2* and *RpBphP3* encode functional bacteriophytochromes, they were co-expressed with the heme oxygenase gene (required for chromophore synthesis) in *E. coli* and subsequently purified. Gel electrophoresis and zinc fluorescence (not shown) demonstrated that the biliverdin molecule was covalently bound in both proteins as previously reported for bacteriophytochromes of various bacterial species (8, 10, 20). Site-directed mutagenesis (data not shown) indicate that the Cys residues of the N terminus, located at position 16 and 28 for *Rp*BphP2 and *Rp*BphP3, respectively, are necessary for attachment of chromophore and are likely to be the site of attachment based upon their position and the

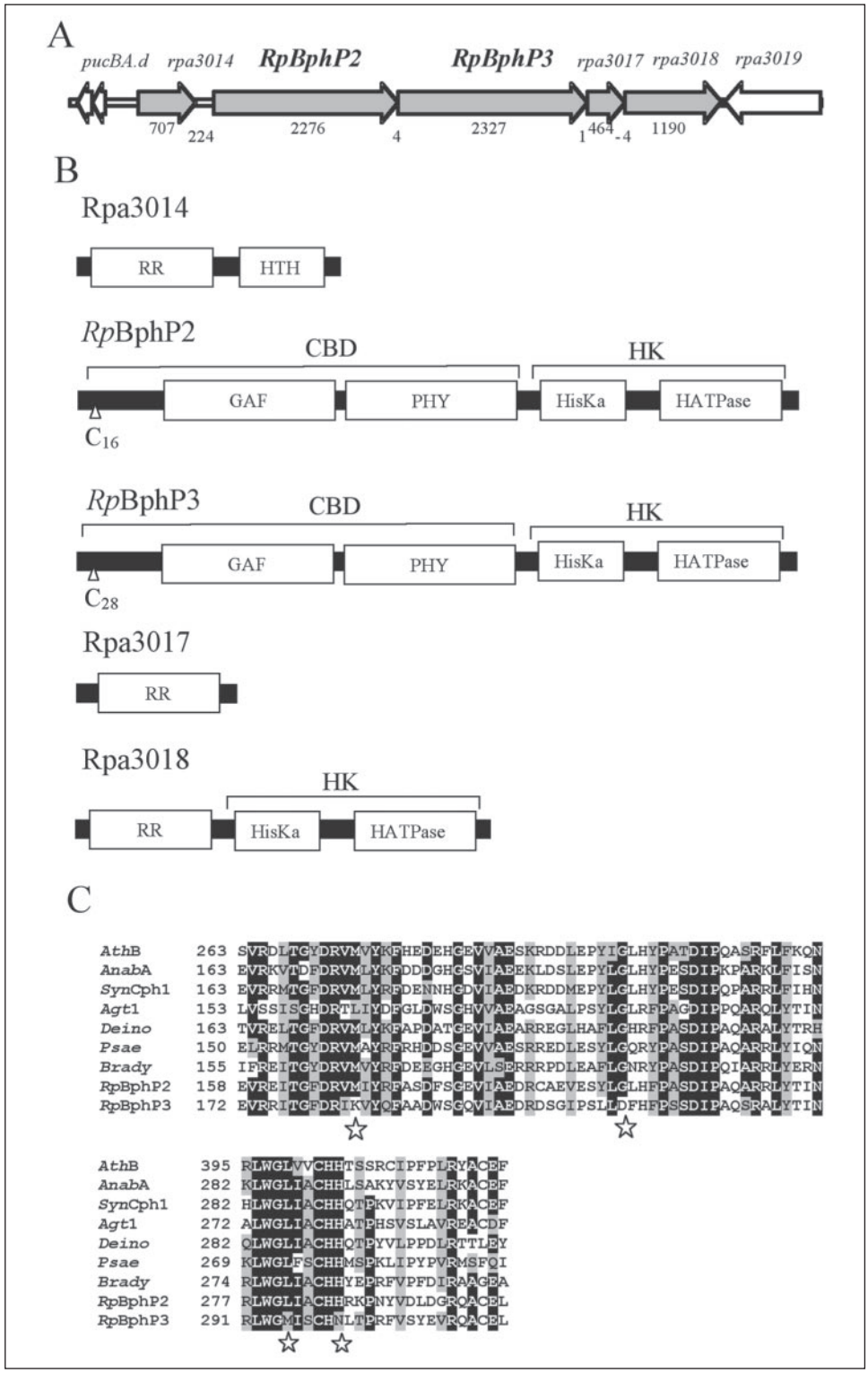

FIGURE 1. **Molecular characterization of *RpBphP2* and *RpBphP3*.** *A*, arrangements of genes located around *RpBphP2* and *RpBphP3*. The genes predicted to belong to the *RpBphP2*/*RpBphP3* operon are in *gray arrows*. The numbers below indicate the size of the open reading frames and of the intergenic regions. *B*, predicted domain structure of Rpa3014, *Rp*BphP2, *Rp*BphP3, Rpa3017, and Rpa3018. The N-terminal cysteine implicated in chromophore binding is indicated by *open triangles*. *HK*, histidine kinase domain; *HisKa*, phosphoacceptor domain; *HATPase*, ATP binding domain; *RR*, response regulator domain, *HTH*, helix-turn-helix domain. *C*, peptide alignment (Clustal X) of two conserved subregions of the CBD. *Ath*B, *Arabidopsis thaliana* PhyB [SW PHYB_ARATH]; *Anab*A, *Anabaena* sp. CphA [SW PHYA_ANASP]; *Syn*Cph1, *Synechocystis* sp. Cph1 [SW PHY1_SYNY3]; *Agt*1, *Agrobacterium tumefaciens At*BhP1 [SPT Q8UDX6]; *Deino*, *Deinococcus radiodurans* [SW BPHY_DEIRA]; *Psae*, *Pseudomonas aeruginosa* [SW BPHY_PSEAE]; *Brady*, *Bradyrhizobium* sp. ORS278 [SPT Q8VUB6]; *Rp*BphP2, *Rps palustris* CGA009 3015 [GenPept g39649933]. *Rp*BphP3, *Rps palustris* CGA009 3016 [GenPept g39649934]. Strictly conserved residues and residues conserved more than 70% are highlighted in *black* and *gray*, respectively. Residues that were mutated in this study are indicated by a *star*.

previous data from the bacteriophytochrome Agp1 of *Agrobacterium* (20).

Absorption and Photochemical Properties—Unexpectedly, the purified *Rp*BphP2 and *Rp*BphP3 bacteriophytochromes present slightly different colors (Fig. 2*A*). The absorption spectra of dark-adapted samples of *Rp*BphP2 and *Rp*BphP3 are typical of the Pr form with a main band centered at 710 and 705 nm, respectively (Fig. 2, *C* and *D*). Both *Rp*BphP2 and *Rp*BphP3 behave as usual bacteriophytochromes assuming a Pr ground state after dark adaptation. This behavior is at variance to that reported for the first bacteriophytochrome (*Rp*BphP1) studied in *Rps. palustris*, which was shown to be stable under its Pfr form (8, 11). Presence of two bacteriophytochromes which differ by their dark-adapted state has also been reported in *Agrobacterium tumefaciens* (21). In this bacterium, the ground state of the bacteriophytochrome *At*BphP1 is the Pr state, whereas the Pfr form of *At*BphP2 corresponds to its dark-adapted state (21). Upon illumination with a 705-nm light of *Rp*BphP2 (Fig. 2*C*), a typical Pr/Pfr transition is observed with the partial bleaching of the main absorption band and appearance of a broad band cen-

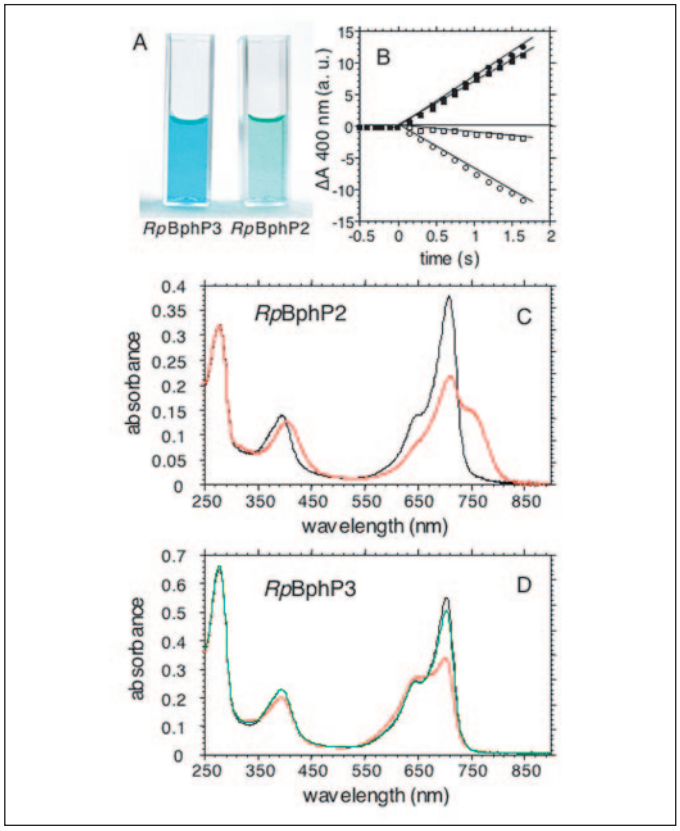

FIGURE 2. **Spectral characterization of recombinant *Rp*BphP2 and *Rp*BphP3.** *A*, picture of samples of *Rp*BphP2 and *Rp*BphP3 in spectrophotometer cuvettes. *B*, initial rates of the phototransformation of Pr into Pnr (*open squares*) and of Pnr into Pr (*closed squares*) for *Rp*BphP3. As a comparison the initial rates of the phototransformation of Pr into Pfr (*open circles*) and of Pfr into Pr (*closed circles*) are shown for *Rp*BphP2. The light-induced absorbance changes were measured at 400 nm. Light excitation was provided by LEDs emitting at 645, 705, and 750 nm. *C*, absorption spectra of recombinant *Rp*BphP2: dark-adapted sample (*black line*), after photoconversion by 705-nm light (*red line*). *D*, absorption spectra of recombinant *Rp*BphP3: dark-adapted sample (*black line*), after photoconversion by 705-nm light (*red line*) or 645-nm light (*green line*).

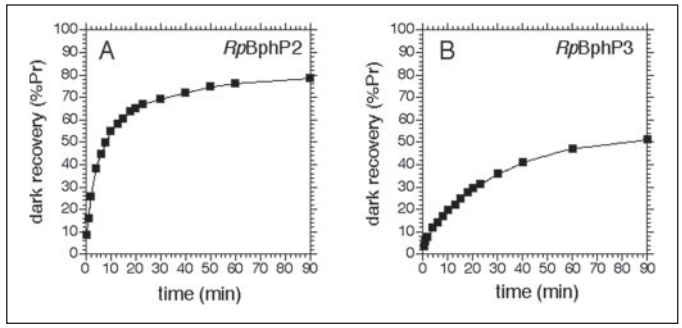

FIGURE 3. **Dark reversion of *Rp*BphP2 and *Rp*BphP3 after a 705 nm illumination.** Absorbance changes occurring in the dark after a 705-nm illumination have been measured at 705 nm and compared with samples dark-adapted for 3 h. *A*, *Rp*BphP2; *B*, *Rp*BphP3.

tered at 750 nm (Fig. 2*C*). Illumination with a 750-nm light restores the dark-adapted spectrum. Dark reversion from the Pfr to the Pr state is a slow process, which requires several tens of minutes (Fig. 3*A*). Unexpectedly, illumination with the 705-nm light on a dark-adapted sample of *Rp*BphP3 (Fig. 2*D*) leads to a large decrease of the main absorption band at 705 nm, but no concomitant absorption band develops in the infrared region. In addition, the shoulder at 650 nm of the Pr form, which corresponds to the vibrational transition of the S1 state, is not bleached. On the contrary, a minor increase in absorption is observed in this wavelength region. This suggests that the 705-nm illumination has induced a new form characterized by an absorption band centered around 650 nm. In agreement with this hypothesis, a fast and near complete reversion to the dark-adapted state is observed when the 705-nm illumination is followed by excitation with a 645-nm light (Fig. 2*D*). In the absence of 645-nm illumination, reversion to the dark-adapted state is very slow. Total dark reversion requires more than 2 h (Fig. 3*B*).

The near complete reversion of *Rp*BphP3 to the dark-adapted state by the 645-nm light (Fig. 2*D*) implies a large difference in quantum yield for the two photoreversible reactions. This difference in quantum yield between the two forms of *Rp*BphP3 is also evidenced by the measurement of the initial rate of Pr formation per absorbed photon upon illumination by a 645-nm light, which is ~6-fold faster than the one measured for the photoconversion under 705-nm illumination (Fig. 2*B*). This behavior is different from that observed for *Rp*BphP2 where the initial rates of the phototransformation of Pr into Pfr and of Pfr into Pr are similar (Fig. 2*B*). Note that these initial rate measurements, determined in the first 2 s of illumination, are not affected by the dark reversion of *Rp*BphP2 and *Rp*BphP3, which takes several tens of minutes in both cases (Fig. 3). The ratio between these initial rates is therefore a good estimate of the ratio of the quantum efficiencies of the photoconversion of the two photoconvertible states.

To determine the absolute absorption spectra of the two photoconvertible forms of *Rp*BphP2 and *Rp*BphP3, we have used the following method. The steady-state spectrum $S_1(\lambda)$ obtained under illumination at a given wavelength, λ_1, is a mixture of the spectra $S_A(\lambda)$ and $S_B(\lambda)$ of the two pure photoconvertible forms, with relative weights $\alpha(\lambda_1)$ and $[1 - \alpha(\lambda_1)]$, respectively,

$$S_1(\lambda) = \alpha(\lambda_1)\, S_A(\lambda) + [1 - \alpha(\lambda_1)]\, S_B(\lambda) \qquad \text{(Eq. 1)}$$

The steady-state condition implies

$$\rho_A\, \alpha(\lambda_1)\, S_A(\lambda_1) = \rho_B\, S_B(\lambda_1)\, [1 - \alpha(\lambda_1)] \qquad \text{(Eq. 2)}$$

where the ρs stand for the quantum efficiencies for the conversion into the other form.

From Equation 1,

$$S_B(\lambda) = [S_1(\lambda) - \alpha(\lambda_1) S_A(\lambda)]/[1 - \alpha(\lambda_1)] \qquad \text{(Eq. 3)}$$

and from Equation 2,

$$S_B(\lambda_1) = \frac{\alpha(\lambda_1)}{1 - \alpha(\lambda_1)} \eta S_A(\lambda_1) \qquad \text{(Eq. 4)}$$

where $\eta = \rho_A/\rho_B$.

Making $\lambda = \lambda_1$ in Equation 3 and equating with Equation 4, one obtains the relation between α and η,

$$\alpha(\lambda_1) = \frac{S_1(\lambda_1)}{S_A(\lambda_1)} \frac{1}{(1 + \eta)} \qquad \text{(Eq. 5)}$$

If $S_A(\lambda)$ (dark-adapted spectrum) and $S_1(\lambda)$ (under steady-state illumination at $\lambda = \lambda_1$) are known, then $\alpha(\lambda_1)$ is a unique function of the ratio of quantum efficiencies $\eta = \rho_A/\rho_B$. Thus, the determination of $S_B(\lambda)$ requires one additional information that may be (i) an independent measurement of ρ or (ii) the acquisition of a steady-state spectrum under actinic illumination at another wavelength λ_2. The first method was applied to both *Rp*BphP2 and *Rp*BphP3 bacteriophytochromes. The measurement of $\eta \approx 1$ for *Rp*BphP2 (Fig. 2*B*), implies that the S_{705} spectrum of Fig. 2*C* is contributed by α (705) ≈ 30% of the Pr form. The corresponding $S_B(\lambda)$ spectrum, *i.e.* the absorption spectrum of the Pfr form is shown in Fig. 4*A*. For *Rp*BphP3, using $\eta \approx 6$ (Fig. 2*B*), we found

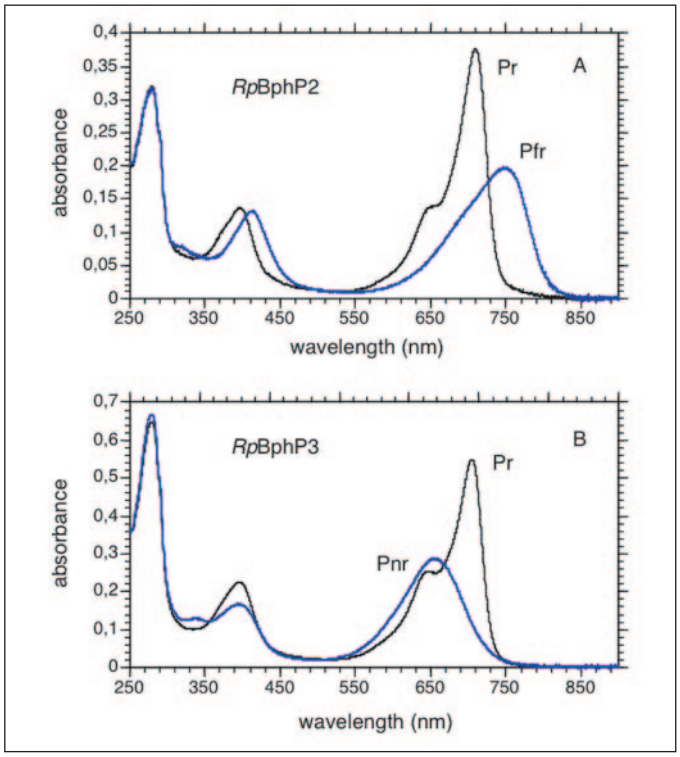

FIGURE 4. **Absorption spectra of recombinant *Rp*BphP2 and *Rp*BphP3.** *A*, *Rp*BphP2. The Pr spectrum (*black line*) corresponds to the dark-adapted sample. The Pfr spectrum (*blue line*) was derived from the spectrum recorded under 705 nm illumination (Fig. 2) using a Pfr/Pr ratio of 0.70 as described in the text. *B*, *Rp*BphP3. The Pr spectrum (*black line*) corresponds to the dark-adapted sample. The Pnr spectrum (*blue line*) was derived from the spectrum recorded under 705 nm illumination (Fig. 2) using a Pnr/Pr ratio of 0.50 as described in the text.

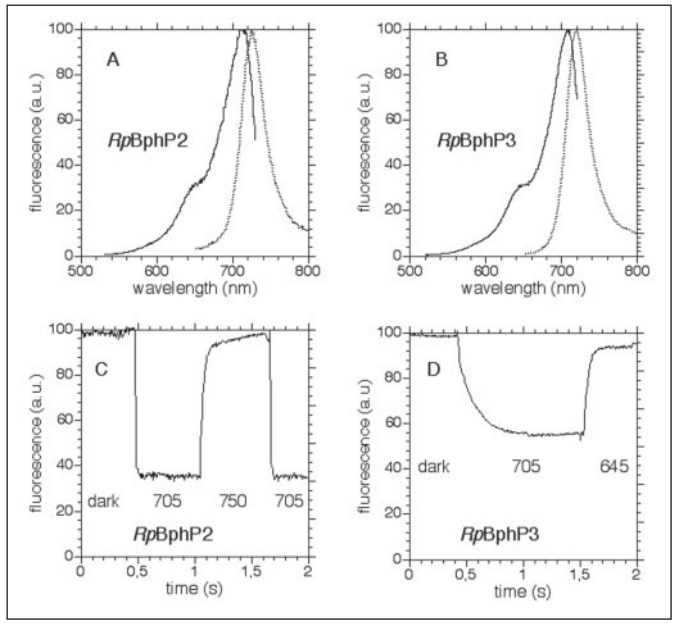

FIGURE 5. **Fluorescent properties of recombinant *Rp*BphP2 and *Rp*BphP3.** *A*, excitation (*solid line*) and emission (*dotted line*) spectra of a sample of *Rp*BphP2 recorded at room temperature. *B*, same as *A* but for a sample of *Rp*BphP3. *C* and *D*, light-induced variations of the fluorescence yield for *Rp*BphP2 (*C*) and *Rp*BphP3 (*D*). The fluorescence emission is measured at 730 nm upon excitation with 400-nm light. The fluorescence yield is measured in the dark or under 705, 645, or 750 nm illumination as indicated. *a.u.*, arbitrary units.

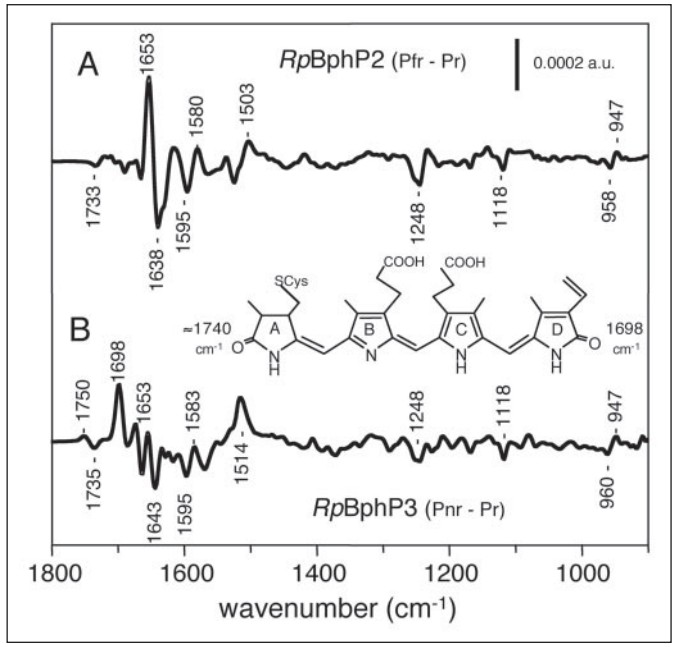

FIGURE 6. **Light-induced FTIR difference spectra of *Rp*BphP2 and *Rp*BphP3.** Light-induced FTIR difference spectra corresponding to the formation of the Pfr form of *Rp*BphP2 (*A*) and to the Pnr form of *Rp*BphP3 (*B*). These spectra are the result of successive light-cycles, applying 705-nm light to generate Pfr (or Pnr) and 750 nm light or 645 nm light to restore the Pr form of *Rp*BphP2 or *Rp*BphP3, respectively. *Inset*, structure of the biliverdin chromophore. *a.u.*, arbitrary units.

that the S_{705} spectrum of Fig. 2*D* is contributed by $\alpha(705) \approx 50\%$ of the Pr form. Using method (ii) for *Rp*BphP2 with the spectra obtained under steady-state illumination at $\lambda_1 = 705$ nm and $\lambda_2 = 645$ nm (Fig. 2*D*), we confirmed a value 6 of for η. The pure $S_B(\lambda)$ spectrum of *Rp*BphP3 shown in Fig. 4*B*.

The absorption spectra of the pure Pr and Pfr forms of *Rp*BphP2 are typical of bacteriophytochromes described so far (8, 10). As already mentioned, the dark-adapted state of *Rp*BphP3 is similar in shape to the Pr state of *Rp*BphP2, *i.e.* a classical Pr spectrum. On the other hand, the light-induced state of *Rp*BphP3 absorbs maximally at 650 nm. The absorption spectrum of this state is similar in shape to the Pfr state of *Rp*BphP2 but blue-shifted by 95 nm (Fig. 4*B*). Because of its peak location, we name this new spectral form Pnr for pigment absorbing in the near red.

In conclusion, *Rp*BphP3 presents unusual photochemical properties in terms of both quantum yield for photoconversion and wavelength position of the Pnr state.

Chromophore Conformation and Transient States—The new optical properties of the short wavelength state of *Rp*BphP3 poses the problem of the biliverdin conformation in this state and the dark-adapted state. High similarities can be found between the dark-adapted state of *Rp*BphP3 and the classical Pr state of *Rp*BphP2 and accordingly between the classical Pfr state and the new Pnr state of *Rp*BphP3. A first argument comes from the almost identical absorption spectra of the two dark-adapted states of these bacteriophytochromes (Fig. 4). A second argument is the observation that the dark-adapted states of both *Rp*BphP2 and *Rp*BphP3 are fluorescent. The fluorescence excitation spectra of *Rp*BphP2 and *Rp*BphP3 closely match their respective absorption spectra, and the emission spectra are centered at 725 and 720 nm, respectively (Fig. 5, *A* and *B*). On the other hand, a large fluorescence decrease occurs upon 705 nm illumination in both cases. This is shown in Fig. 5, *C* and *D* where the fluorescence yield of both bacteriophytochromes have been measured in the dark or under 705-nm illumination. The decreases in fluorescence yield, ~65 and 45% for *Rp*BphP2 and *Rp*BphP3, respectively (Fig. 5, *C* and *D*), correspond nicely to the amounts of Pfr and Pnr states formed under such illumination (Fig. 2). The non-fluorescent character of the new Pnr state of *Rp*BphP3 is a typical prop-

erty of the "classical" Pfr form of phytochromes (22). A third argument comes from the comparison of the FTIR difference spectra recorded with both bacteriophytochromes. The Pfr − Pr FTIR difference spectrum recorded with *Rp*BphP2 (Fig. 6*A*) presents a striking similarity to that observed for the plant phytochrome (23, 24) for which ZZZ to ZZE isomerization in C_{15} of phytochromobilin was demonstrated using NMR spectroscopy. The occurrence of common infrared bands at 1653/1643–1638, 1248, 1118, 960–958/947 cm^{-1} and especially at 1595/1583 cm^{-1} in the Pnr-Pr and Pfr-Pr spectra recorded with *Rp*BphP3 or *Rp*BphP2 strongly supports that Z to E isomerization also occurs around the $C_{15}=C_{16}$ double bond for *Rp*BphP3. Previous studies on phytochromes using chromophores chemically modified at ring D or ^{18}O-labeled at ring A have shown that the contributions of the carbonyl group of ring A lie above 1730 cm^{-1}, whereas those of ring D are at 1710–1696 cm^{-1} (24). Thus we assign the upshift of 1735–1750 cm^{-1} upon Pr to Pnr transition to ring A carbonyl, whereas the large positive band at 1698 cm^{-1} is assigned to the carbonyl group of ring D in the Pnr form of *Rp*BphP3 (Fig. 6). The last argument comes from the analysis of the flash-induced absorption changes following an exciting flash. Fig. 7*A* shows the light-induced absorbance changes detected at different times, between 1 and 100 ms, after flash excitation of a dark-adapted sample of *Rp*BphP2. The light-induced difference spectrum detected 1 ms after the exciting flash presents an absorbance increase centered at 740 nm and a bleaching around 640 and 705 nm. When the light-induced absorbance changes are detected at longer times, a shift to longer wavelengths is observed for the positive changes together with an increase of the amplitude of the negative changes (Fig. 7*A*). These light-induced changes can be interpreted as follows. Flash excitation induces the formation of a short-lived state absorbing around 740 nm, which is transformed with a half-time of 10 ms (Fig. 7*A*, *inset*) into the stable Pfr state absorbing around 760 nm. The properties of this transient state, in terms of half-time and absorption at shorter wavelength than the stable Pfr form, are similar to the lumi-R state observed for plant phytochrome (22, 25). An equivalent transitory state is observed upon phototransformation from the Pr to the Pnr state in the case of *Rp*BphP3 (Fig. 7*B*). This short lived state peaks around 730 nm and is converted into the stable Pnr form with a half-time of 10 ms. On the other hand, we have observed no transition state, in the ms to second time range, for both the flash-induced transformation of Pfr into Pr or Pnr into Pr for *Rp*BphP2 and *Rp*BphP3, respectively (data not shown). We take the similarity between the transient states measured in *Rp*BphP2 and *Rp*BphP3 as supplementary evidence that their dark-adapted states correspond to a Pr state. Collectively, the above results strongly support an identical conformational state of the chromophore for the new Pnr form of *Rp*BphP3 and the classical Pfr form of *Rp*BphP2. We therefore propose that the new Pnr form of *Rp*BphP3 is equivalent to the classical Pfr but absorbing at much shorter wavelengths.

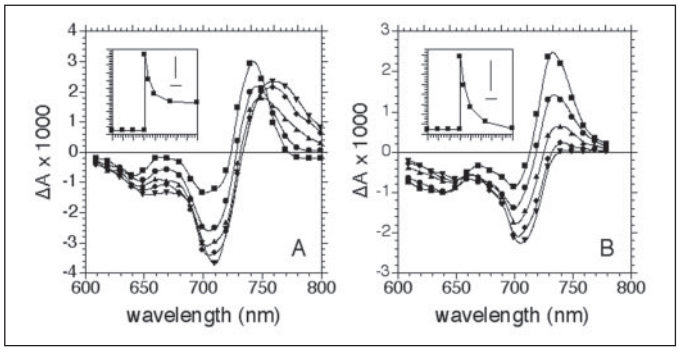

FIGURE 7. **Flash-induced absorption difference spectra of *Rp*BphP2 and *Rp*BphP3.** Flash-induced absorption difference spectra corresponding to the formation of the Pfr form of *Rp*BphP2 (*A*) and to the Pnr form of *Rp*BphP3 (*B*). Flash-induced absorption changes were detected at different times (*squares*, 1 ms; *circles*, 8 ms; *triangles*, 20 ms; *diamonds*, 50 ms; *inverted triangles*, 100 ms) after a short (2 μs) excitation flash. The *insets* correspond to the kinetics of the absorbance changes detected at 740 nm. The *vertical* and *horizontal bars* represent $\Delta A = 10^{-3}$ and 20 ms, respectively.

Autophosphorylation and Phosphotransfer—Both *Rp*BphP2 and *Rp*BphP3 bacteriophytochromes possess a histidine kinase module at their C-terminal regions (Fig. 1*B*). We have determined the correlation between this kinase activity and their conformational states by incubation in the presence of [γ-^{32}P]ATP. Both bacteriophytochromes autophosphorylate in the dark, *i.e.* under their Pr forms (Fig. 8*A*). In agreement with His serving as phosphoacceptor site, the autophosphorylated *Rp*BphP2 and *Rp*BphP3 are acid labile and base stable (data not shown). Illumination of *Rp*BphP2 with a 705-nm light strongly represses its kinase activity indicating that its Pfr form is not able to autophospho-

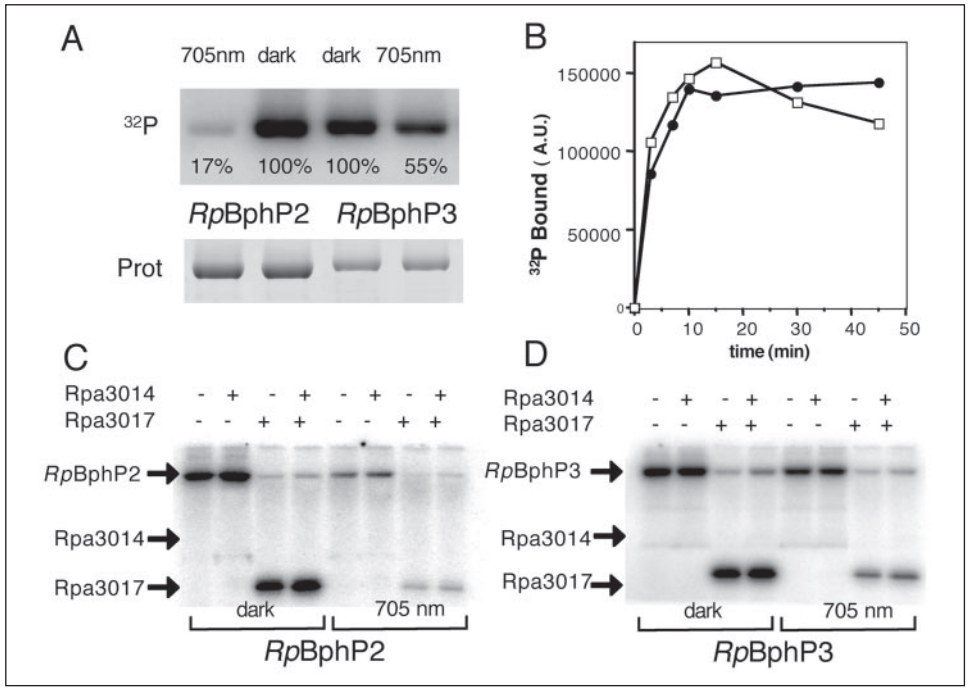

FIGURE 8. ***Rp*BphP2 and *Rp*BphP3 act as light-regulated histidine kinases.** *A*, autophosphorylation of purified *Rp*BphP2 and *Rp*BphP3 in the dark or under illumination at 705 nm. After incubation with [γ-^{32}P]ATP during 1 h, the reaction products were separated by SDS-PAGE, and the gels were subjected to autoradiography (*top*) or stained for protein (*prot*) with Coomassie Blue (*bottom*). Percentages of phosphorylation levels are indicated below the autoradiogram. *B*, kinetics of phosphotransfer between the two bacteriophytochromes and the response regulator Rpa3017. *Open squares*, *Rp*BphP2; *filled circles*, *Rp*BphP3. *C* and *D*, transfer of the phosphate from *Rp*BphP2 (*C*) and *Rp*BphP3 (*D*) to the response regulators Rpa3014 and Rpa3017. *A.U.*, arbitrary units.

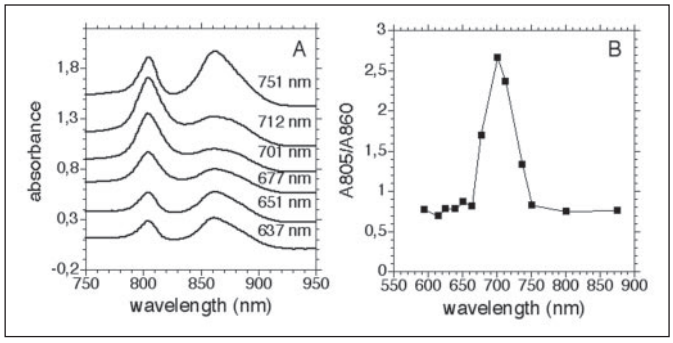

FIGURE 9. **Effect of light of various wavelengths on the LH4 synthesis.** *A*, absorption spectra of *Rps. palustris* cells grown under semiaerobic conditions subjected to illumination at various wavelengths (from 637 to 751 nm) provided by LEDs. The light intensity was set to 10 μmol of photon/m^2/s for each wavelength. *B*, variation of the ratio A805/A860 as a function of the wavelength of the incident light, deduced from experiments similar to those reported in part *A*.

rylate. Excitation with a 705-nm light induces a 45% decrease of the level of phosphorylation in the case of *Rp*BphP3. This value is very close to the amount of state Pnr formed under this light condition (Fig. 2*D*), indicating that the Pnr form of *Rp*BphP3 displays probably no kinase activity.

We next investigated whether the Pr forms of *Rp*BphP2 and *Rp*BphP3 could transfer their phosphates to the response regulators Rpa3014 and Rpa3017, whose genes are located on both sides of *RpBphP2* and *RpBphP3* (Fig. 1, *A* and *B*). A rapid and efficient phosphotransfer was observed from both bacteriophytochromes to Rpa3017 (Fig. 8, *B–D*), indicating that this response regulator is a common element of the signaling pathways initiated by *Rp*BphP2 and *Rp*BphP3. In contrast, although the prediction of a helix-turn-helix DNA binding domain in Rpa3014 suggests that this response regulator could be the last element of the transduction pathway of *Rp*BphP2 and *Rp*BphP3, no phosphotransfer was observed from these bacteriophytochromes to Rpa3014, even in the presence of Rpa3017 (Fig. 8, *C* and *D*). We cannot exclude at the moment that this lack of phosphotransfer is because of an incorrect folding of the recombinant Rpa3014 protein. Another explanation could be that additional partners are implicated in the phosphotransfer from *Rp*BphP2 or *Rp*BphP3 to Rpa3014, via Rpa3017. One of these partners could be the response regulator containing also a histidine-kinase domain, encoded by the *rpa3018* gene found just downstream of *rpa3017* (Fig. 1, *A* and *B*). Experiments to complete the characterization of this complex light signaling pathway are in progress.

Action Spectrum of LH4 Synthesis and Phenotypes of RpBphP2 and RpBphP3 Deletion Mutants—To optimize their metabolism according to environmental changes, photosynthetic bacteria regulate the expression level and composition of their photosystems by means of highly sophisticated mechanisms. In the case of *Rps. palustris*, growth under low light intensity under anaerobic condition results in the enhancement of the synthesis of LH4 complexes encoded by the *pucBAd* genes and a decrease of LH2 complexes encoded by the other *pucBA* genes (14, 15). The *pucBAd* genes are located upstream the *RpBphP2* and *RpBphP3* genes. Based on these genes arrangement and the ability of *Rp*BphP2 and *Rp*BphP3 to phosphorylate the same response regulator, one appealing hypothesis is to suppose that these two bacteriophytochromes are involved in the regulation of the LH4 complexes.

To test this hypothesis, *Rps. palustris* CEA001 was subjected to illumination at various wavelengths provided by LEDs emitting between 590 and 875 nm. The experiment was performed under semiaerobic condition because of the requirement for oxygen in the bacteriophytochrome chromophore synthesis. Fig. 9*A* shows the absorption spectra of cells grown under some selected wavelengths. Clearly, the relative amount between the LH4 complexes and the LH2 complexes depends highly upon the illumination wavelength. The ratio between the absorptions at 805 and 860 nm (A805/A860), which is a relative measure of the ratio between LH4 and LH2 complexes, is shown in Fig. 8*B*. The synthesis of the LH4 complexes, concomitant with a decrease in LH2 complexes, is specifically enhanced for wavelengths comprised between 680 and 730 nm with a maximum around 705–710 nm (Fig. 9*B*). This wavelength range corresponds precisely to illumination for which *both Rp*BphP2 and *Rp*BphP3 are predominantly under their non-phosphorylated states, Pfr and Pnr forms (Fig. 8*A*). Indeed, on the one hand, illumination with wavelengths longer than 740 nm, not absorbed by the dark Pr forms of both *Rp*BphP2 and *Rp*BphP3, does not modify the phosphorylation state of these bacteriophytochromes, which both remain phosphorylated. On the other hand, excitation with wavelengths shorter than 670 nm converts *Rp*BphP2 to its non-phosphorylated Pfr form but maintains *Rp*BphP3 predominantly in its phosphorylated Pr state (Figs. 2 and 8).

Because the enhancement of LH4 complexes synthesis has been reported to occur only at very low light intensity under anaerobic conditions (15), we have followed the LH4 synthesis as a function of the intensity of 710 nm light. This enhancement was half-saturated for intensity of 5 μmol of photon/m^2/s and remained constant up to 200 μmol of photon/m^2/s (not shown). This unexpected behavior is probably because of the difference in growth conditions between the present work (semiaerobic) and the previous report (anaerobic) (15).

Because of the peculiar absorption and quantum yield properties of the *Rp*BphP3 Pnr state, we expect that both bacteriophytochromes are in their dephosphorylated activating state only when the 710-nm light is in excess to 645-nm light. To test this possibility the synthesis of LH4 complexes has been measured as a function of the ratio between 645 and 710 nm light intensities. We indeed observed that increasing this ratio led to a large decrease in the synthesis of LH4 complexes. Typically, the ratio A805/A860 decreases from 2.0 to 1.2 when the ratio between 645 and 710 nm light intensities increases from 0.1 to 10 (not shown).

To definitively prove that the LH4 synthesis is regulated by the action of *Rp*BphP2 and *Rp*BphP3, we have examined the phenotype of mutants deleted in *RpBphP2* or *RpBphP3* genes. In contrast to the wild-type strain, no synthesis of LH4 complexes was observed for these mutants irrespective of the illumination intensity and wavelength (not shown).

DISCUSSION

Based on the results described above, we conclude that the light-induced dephosphorylation of *Rp*BphP2 and *Rp*BphP3 is the first step of the signal transduction pathway of the LH4 synthesis. These two bacteriophytochromes act as the inputs to an "and gate" for the regulation of the LH4 synthesis as a function of the relative intensities of 645 and 710 nm light. We propose that measurement of this ratio is an indirect detection of the presence of phytoplankton. Indeed, in their natural environment, photosynthetic bacteria may develop below dense layers of phytoplankton. Because of the strong absorption of cyanobacteria and microalgae chromophores in the visible region up to 700 nm, the ratio of photons of 645 and 710 nm reaching the lower layer of photosynthetic bacteria is significantly affected by the presence of phytoplankton. In particular, photosynthetic bacteria receive only far-red light in these conditions. This significantly decreases their available light energy. To overcome this limitation in light supply, *Rps. palustris* activates the synthesis of LH4 complexes, via the action of *Rp*BphP2 and *Rp*BphP3 and decreases the synthesis of LH2 complexes. These changes in LH complexes significantly enhance the light capture efficiency of the bacteria. First, the infrared absorption of all the bacteriochlorophyll molecules of the LH4 complexes is centered around 800 nm, whereas

most (two-thirds) of the absorption the LH2 complexes peaks at longer wavelengths, around 860 nm (15). Because much more light is transmitted at 800 nm than around 860 nm due to depth water attenuation (26), the LH4 complexes collect more light than the LH2 complexes. In addition, the increase in energy gap between LH4 (B800 LH2) and the B870 LH1 complexes, as compared with the gap between LH2 (B800-850 LH2) and B870 LH1, constitutes an effective sink and a barrier against back transfer of excitonic energy.

The strategy adopted by *Rps. palustris* to measure the difference in intensity and light quality has been the involvement of a pair bacteriophytochromes, one of which, *Rp*BphP3, presents atypical optical properties. Unusual photochemical properties have also been reported recently for the light sensor protein Ppr of *Rhodospirillum centenum* by Kyndt *et al.* (27). This chromoprotein possesses both a photoactive yellow protein domain and a bacteriophytochrome domain (5). The dark-adapted form of Ppr presents an absorption maximum at 702 nm with a shoulder around 650 nm, typical of the Pr form of bacteriophytochromes. Upon illumination, both the 702- and the 650-nm transitions bleach with no concomitant appearance of a red- or blue-shifted transition (27). It is important to note that this behavior, which may appear at first sight similar to what we observed for *Rp*BphP3, corresponds to a real bleaching of the optical transitions of Ppr and not to a blue shift of these transitions as in the case of *Rp*BphP3 (Fig. 4*B*).

Another example of unusual spectral properties has been also reported for the PixJ1 holoprotein of the cyanobacterium *Synechocystis* sp. PCC6803 (28). This light sensor shows a photoreversible conversion between a blue light-absorbing form and a green light-absorbing form. However this chromoprotein contains two GAF domains but does not possess the CBD, characteristic of phytochromes. In addition, the chemical nature of the chromophore remains unknown. It has been shown to be different from the various phytochrome chromophores previously characterized in plant, cyanobacteria or bacteria (phytochromobilin, phycocyanobilin, biliverdin, respectively) (28). So PixJ1 cannot be considered as a *bona fide* phytochrome.

The short wavelength position of the Pnr form of *Rp*BphP3 may be related to a less extensive conjugation of the π-electrons because of the distortion of one of the biliverdin ring. In agreement with this hypothesis, the large positive absorption band at 1698 cm^{-1}, assigned to the carbonyl group of ring D in the Pnr form of *Rp*BphP3 (Fig. 6) may indicate a difference in the environment of this carbonyl between *Rp*BphP3 and *Rp*BphP2. This could be because of a modification of the coupling of ν(C=O) and ν(C=C) modes (of the C_{15}=C_{16} methine bridge) in the Pnr state of *Rp*BphP3. Sequence alignment of several bacteriophytochromes reveals unconserved amino acids in the CBD of *Rp*BphP3 (Fig. 1*C*). Some of these residues were introduced in *Rp*BphP2 by site-directed mutagenesis (Fig. 1*C*), to test whether this could confer the short wavelength position of the Pnr form of *Rp*BphP3 to *Rp*BphP2. This was not the case with any of these single mutations. The molecular basis of the short wavelength position of the new Pnr form remains therefore to be disclosed. Construction of mutants containing multiple amino acids substitutions is in progress to address this question.

Several questions concerning the molecular mechanism of the light regulation of LH4 complexes remain to be answered. What other partner(s) are involved in the phosphorelay initiated by the two bacteriophytochromes *Rp*BphP2 and *Rp*BphP2? Putative candidates are the transcriptional factor Rpa3014 and the response regulator Rpa3018, whose genes belong to the same operon than *RpBphP2* and *RpBphP3*. These two proteins present some similarities with the transcriptional factor Rpa1491 and the putative *Rp*BphP4 bacteriophytochrome, respectively. The *RpBphP4* and *rpa1491* genes are located near the *pucBAe* genes encoding LH2 complexes. A cross-talk between the bacteriophytochrome *Rp*BphP4 and the three proteins, Rpa3014, Rpa3018, and Rpa1491, is possibly involved in the co-regulation of the synthesis of the LH2 and LH4 complexes. Although the genes of the two other bacteriophytochromes, present in *Rps. palustris*, are found in genome regions noticeably distant from photosynthesis genes, we cannot exclude yet their participation in the regulation of the synthesis of the photosynthetic apparatus. Another point to be solved is the mechanism of the enhancement of the LH4 complexes synthesis observed only at low light intensity under anaerobic conditions, for which the involvement of *Rp*BphP2 or *Rp*BphP3 is difficult to understand, because their chromophore synthesis requires oxygen.

The measurement of light parameters, like those described above for *Rps. palustris*, is essential for photosynthetic organisms for the adaptation to their light environment to regulate light capture for an optimal photosynthetic activity. Changes in pigment composition in response of different wavelengths, the so-called complementary chromatic adaptation, has been observed in different species of cyanobacteria. For example, the pigmentation of cyanobacteria changes in function of light quality. In *Fremyella diplosiphon*, red light (≈650 nm) induces the synthesis of a large amount of blue-absorbing phycocyanin biliprotein but only small amount of the red-absorbing phycoerythrin biliprotein (29, 30). In contrast, green light (≈540 nm) induces the synthesis of large quantities of phycoerythrin but only small amounts of phycocyanin. The regulation observed during this complementary chromatic adaptation suggests the existence of a peculiar light control system. This system presents therefore some homologies to the light-sensing system of regulation of LH4 complexes of *Rps. palustris*. The peculiar light sensors required for complementary chromatic adaptation would have to absorb in the green (540 nm) and the red (650 nm) regions. It has been recently proposed that the photoreceptor RcaE is required for both green and red light responsiveness during complementary chromatic adaptation (31). This protein contains both the CBD and the transmitter module typical of phytochrome (3). Although it has been shown that RcaE covalently binds *in vitro* classical bilins (phycocyanobilin, phytochromobilin, biliverdin), the reconstituted proteins obtained are not photochromics suggesting that contrary to plant or bacterial phytochromes, RcaE could require a separate lyase activity for an accurate bilin attachment (31). In the absence of spectral analysis, it is still unclear whether complementary chromatic adaptation-regulated gene expression in *Fremyella* is under the control of RcaE alone with unusual optical properties. Alternatively, RcaE could be associated in tandem with another photoreceptor similarly to the organization of *Rp*BphP2/*Rp*BphP3 present in *Rps. palustris*.

Acknowledgments—We thank Drs. B. Genty and B. Dimon for helpful comments. We wish also to express our gratitude to Dr. J. Lavergne for computing the equations of the pure spectra calculation and for constructive discussions.

REFERENCES

1. Smith, H. (2000) *Nature* **407,** 585–591
2. Quail, P. H., Boylan, M. T., Parks, B. M., Short, T. W., Xu, Y., and Wagner, D. (1995) *Science* **268,** 675–680
3. Kehoe, D. M., and Grossman, A. R. (1996) *Science* **273,** 1409–1412
4. Hughes, J., Lamparter, T., Mittmann, F., Hartmann, E., Gärtner, W., Wilde, A., and Börner, T. (1997) *Nature* **386,** 663
5. Jiang, Z.-Y., Swem, L. R., Rushing, B. G., Devanathan, S., Tollin, G., and Bauer, C. E. (1999) *Science* **285,** 406–409
6. Davis, S. J., Vener, A. V., and Vierstra, R. D. (1999) *Science* **286,** 2517–2520
7. Yoshihara, S., Suzuki, F., Fujita, H., Geng, X. X., and Ikeuchi, M. (2000) *Plant Cell Physiol.* **41,** 1299–1304
8. Giraud, E., Fardoux, J., Fourrier, N., Hannibal, L., Genty, B., Bouyer, P., Dreyfus, B., and Verméglio, A. (2002) *Nature* **417,** 202–205
9. Yeh, K. C., Wu, S. H., Murphy, J. T., and Lagarias, J. C. (1997) *Science* **277,** 1505–1508
10. Bhoo, S.-H., Davis, S. J., Walker, J., Karniol, B., and Vierstra, R. D. (2001) *Nature* **414,**

776–779
11. Giraud, E., Zappa, S., Jaubert, M., Hannibal, L., Fardoux, J., Adriano, J.-M., Bouyer, P., Genty, B., Pignol, D., and Verméglio, A. (2004) *Photochem. Photobiol. Sci.* **3,** 587–591
12. Giraud, E., Hannibal, L., Fardoux, J., Jaubert, M., Jourand, P., Dreyfus, B., Sturgis, J. N., and Verméglio, A. (2004) *J. Biol. Chem.* **279,** 15076–15083
13. Tadros, M. H., and Waterkamp, K. (1989) *EMBO J.* **8,** 1303–1308
14. Evans, M. B., Hawthornthwaite, A. M., and Cogdell, R. J. (1990) *Biochim. Biophys. Acta* **1016,** 71–76
15. Hartigan, N., Tharia, H. A., Sweeney, F., Lawless, A. M., and Papiz, M. Z. (2002) *Biophys. J.* **82,** 963–977
16. Larimer, F. W., Chain, P., Hauser, L., Lamerdin, J., Malfatti, S., Do, L., Land, M. L., Pelletier, D. A., Beatty, J. T., Lang, A. S., Tabita, F. R., Gibson, J. L., Hanson, T. E., Bobst, C., Torres, J. L., Peres, C., Harrison, F. H., Gibson, J., and Harwood, C. S. (2004) *Nature Biotech.* **22,** 55–61
17. Kokotek, W., and Lotz, W. (1989) *Gene* (*Amst.*) **84,** 467–471
18. Quandt, J., and Hynes, M. F. (1993) *Gene* (*Amst.*) **127,** 15–21
19. Joliot, P., Béal, D., and Frilley, B. (1980) *J. Chimie Physique* **77,** 209–216
20. Lamparter, T., Michael, N., Mittmann, F., and Esteban, B. (2002) *Proc. Natl. Acad. Sci. U. S. A.* **99,** 11628–11163
21. Karniol, B., and Vierstra, R. D. (2003) *Proc. Natl. Acad. Sci. U. S. A.* **100,** 2807–2812
22. Sineshchekov, V. A. (1995) *Biochim. Biophys. Acta* **1228,** 125–164
23. Foerstendorf, H., Benda, C., Gärtner, W., Storf, M., Scheer, H., and Siebert, F. (2001) *Biochemistry* **40,** 14952–14959
24. Foerstendorf, H., Mummert, E., Schäfer, E., Scheer, H., and Siebert, F. (1996) *Biochemistry* **35,** 10793–10799
25. Linschitz, H., Kasche, V., Butler, W. L., and Siegelman, H. W. (1966) *J. Biol. Chem.* **241,** 3395–3403
26. Vilia, X., Colomer, J., and Garcia-Gil, L. J. (1996) *Ecolog. Model.* **87,** 59–68
27. Kyndt, J. A., Meyer, T. E., and Cusanovich, M. A. (2004) *Photochem. Photobiol. Sci.* **3,** 519–530
28. Yoshihara, S., Katayama, M., Geng, X., and Ikeuchi, M. (2004) *Plant Cell Physiol.* **45,** 1729–1737
29. Bogorad, L. (1975) *Annu. Rev. Plant Physiol.* **26,** 369–401
30. Tandeau de Marsac, N. (1977) *J. Bacteriol.* **130,** 82–91
31. Terauchi, K., Montgomery, B. L., Grossman, A. R., Lagarias, J. C., and Kehoe, D. M. (2004) *Mol. Microbiol.* **51,** 567–577

Metabolism and Bioenergetics:

A New Type of Bacteriophytochrome Acts in Tandem with a Classical Bacteriophytochrome to Control the Antennae Synthesis in *Rhodopseudomonas palustris*

Eric Giraud, Sébastien Zappa, Laurie Vuillet, Jean-Marc Adriano, Laure Hannibal, Joël Fardoux, Catherine Berthomieu, Pierre Bouyer, David Pignol and André Verméglio

J. Biol. Chem. 2005, 280:32389-32397.
doi: 10.1074/jbc.M506890200 originally published online July 11, 2005